Nonlinear Odd Viscoelastic Effect

Ashwat Jain, ^{1,*} Wojciech J. Jankowski, ^{2,†} M. Mehraeen, ¹ and Robert-Jan Slager^{1,2,‡}

¹Department of Physics and Astronomy, University of Manchester, Oxford Road, Manchester M13 9PL, UK

²Theory of Condensed Matter Group, Cavendish Laboratory, University

of Cambridge, J. J. Thomson Avenue, Cambridge CB3 0HE, UK

(Dated: December 1, 2025)

We uncover a class of nonlinear odd viscoelastic effects in three spatial dimensions. We show that these dissipationless effects arise upon combining strains in two orthogonal directions, yielding momentum flow in the third direction. We demonstrate that the effect arises from nontrivial geometric tensors in quantum states, and can be scaled up with integer topological invariants. We further demonstrate that the effect fingerprints the multiband Hilbert-space geometry of underlying quantum states, as encoded in three-state geometric tensors. Our findings unravel the role of multistate geometry in viscoelastic phenomena, paving a path for experimental observation of uncharted nonlinear odd viscoelastic responses in quantum systems.

Introduction.— Viscosity, an emergent property of physical fluids, arises upon perturbing their geometry. Viscous responses, encoded in viscoelastic tensors, are captured by the momentum flow correlators upon applying shears and stresses as geometric perturbations [1–3]. Beyond its distinct emergence in classical fluids ranging from liquid water to honey or glasses, it is further realized by quantum fluids of electrons in crystals. In particular, viscoelastic tensors can also include dissipationless flows of momentum orthogonal to perturbation directions, commonly known as odd viscosity [4–8]. In condensed matter systems, odd viscosity arises in viscous Hall currents, that is as Hall viscosity [9–12]. Odd viscosity has been experimentally measured in crystals such as graphene [13], and was further recognized to contribute corrections to spatially dispersive conductivities [10, 14].

Hall phenomena have, amongst many other impactful directions, been related to two themes of study; first, there is a primary role for topology, well exemplified by various detailed responses of quantum Hall fluids [15–20]. Second, it has been shown in a multitude of works that intrinsic electronic Hall effects occur not only at linear order in perturbing electric fields [21], but are also manifested in higher orders [22–28]. In addition, electronic nonlinear Hall responses are an increasingly studied topic of recent interest in quantum Hall fluids and topological phases, from both experimental and theoretical angles [29–37]. Universally, these responses heavily depend on the Hilbert-space geometry of quantum states, which is intricately linked to, and can be controlled by the topology of wavefunctions [38–43].

The growing insights into the relations between quantum geometry [41, 42, 44–47] and topological and symmetry-indicated invariants in free-fermion systems [48–53] recently culminated in the discovery of uncharted multigap invariants [25, 54–62]. Given the well-

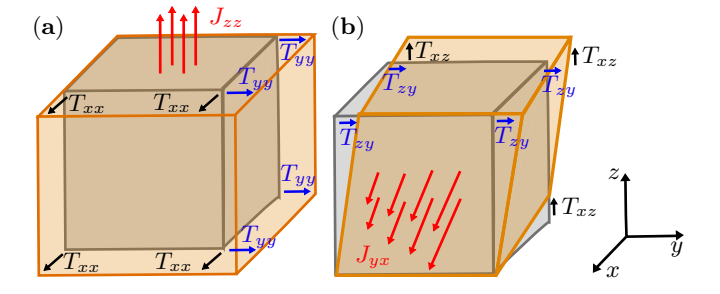


FIG. 1. Nonlinear odd viscoelastic effects. The effects are encoded in the stress tensor correlators $\langle [T_{mn}, [T_{kl}, T_{ij}]] \rangle$ of the electron fluid. (a) Nonlinear elastic response to normal stresses manifested as $\langle [T_{yy}, [T_{xx}, T_{zz}]] \rangle$. (b) Nonlinear viscous response to shear-stress deformations, captured by nontrivial $\langle [T_{zy}, [T_{xz}, T_{yx}]] \rangle$ correlators.

established understanding of these fields, a natural question emerges as to whether this progress galvanizes new insights upon exploiting the relation between multiband geometry, topology, higher-order responses, and odd viscosity. Notably, a nonlinear viscoelastic effect which might accompany electronic Hall currents has, to our knowledge, not been explored in any such multi-state systems, particularly within these geometric frameworks.

In this work, we predict the emergence of such an effect and, in doing so, also address the problem of the existence of nonlinear odd viscoelastic effects (NOVEs) in quantum fluids. We demonstrate that the nonlinear viscous correlators of momentum and stress operators naturally arise in magnetic topological phases, establishing these as strong candidates for measuring viscous nonlinearities. We further show that the NOVEs are uniquely constituted by two-state and three-state quantum geometric tensors, revealing the crucial role of multistate geometry in viscous responses. Furthermore, we demonstrate the interplay of nonlinear viscosity and ground-state topologies via qualitative changes of nonlinear stress correlators, culminating in marked variations of NOVEs across topological phase transitions (TPTs). Finally, we showcase the nonlinear viscoelastic phenomenology via defor-

^{*} ashwat.jain@postgrad.manchester.ac.uk

 $[\]dagger$ wjj25@cam.ac.uk

[‡] robert-jan.slager@manchester.ac.uk

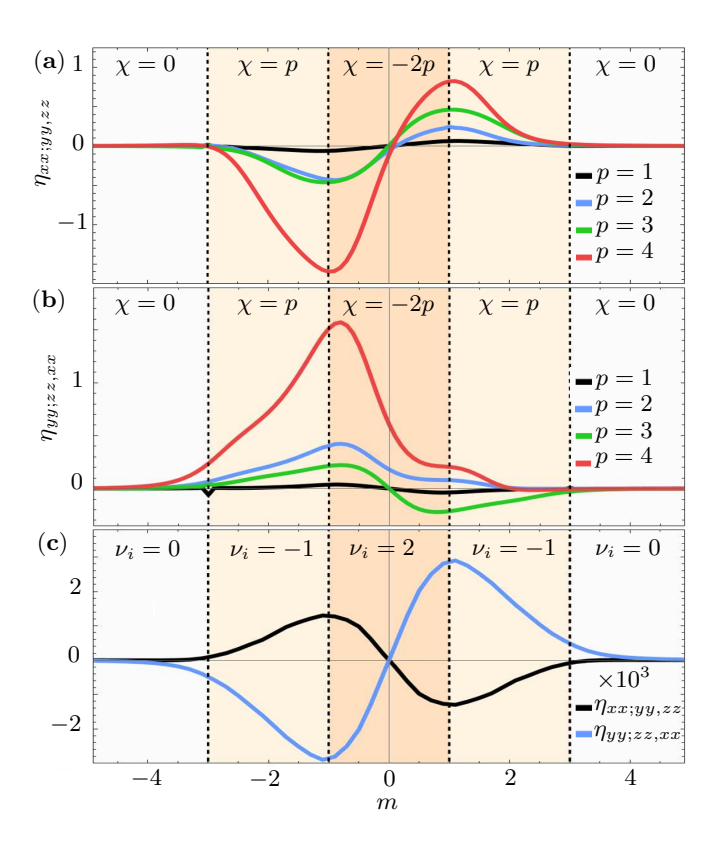


FIG. 2. Two- and three-band contributions to the nonlinear odd viscosity. (a) Two-band $\eta_{xx;yy,zz}$ and (b) Two-band $\eta_{yy;zz,xx}$ for the perturbed MRW model with mass m, show-casing an increasing response strength with the increasing Hopf invariant magnitude $|\chi|$. Here, $p \in \mathbb{Z}$ denotes the momentum scaling factor $k_z \to pk_z$ which leads to scaling of the invariant. (c) Three-band $\eta_{xx;yy,zz}$ and $\eta_{yy;zz,xx}$ realized in a flattened three-dimensional chiral model with chiral invariant $|\nu_i|$ which trivializes upon adding a symmetry-breaking perturbation. The $\eta_{zz;xx,yy}$ response component follows from the sum rule $\eta_{xx;yy,zz} + \eta_{yy;zz,xx} + \eta_{zz;xx,yy} = 0$.

mations of real-space Wannier functions, subject to nonlinear couplings to shears and stresses. Our findings establish a set of unique viscoelastic effects, and experimental protocols to measure them, in a broad range of topological phases of matter. Beyond allowing to access and fingerprint exotic magnetic topological invariants, our results establish uncharted viscoelastic probes of nontrivial multistate geometries for electronic states in solids.

Nonlinear odd viscoelastic response.— To retrieve the NOVE, we begin with deriving an expression for the dc nonlinear viscoelastic response tensor $\eta_{ij;kl,mn}$, with $\{i,j,k,l,m,n\} = \{x,y,z\}$. In particular, $\eta_{ij;kl,mn}$ captures the momentum currents $T_{ij} = \partial H/\partial w_{ij}$ [63] in a system governed by a Hamiltonian H perturbed by the static fields w_{kl} , w_{mn} coupling to stress tensor elements

$$\eta_{ij;kl,mn} \equiv \lim_{\omega \to 0} \frac{\mathrm{i}}{\omega} \langle [T_{mn}, [T_{kl}, T_{ij}]] \rangle. \tag{1}$$

The elastic fields $w_{kl} = \partial u_k/\partial x_l$, which couple to currents T_{kl} , are introduced by deformations $\mathbf{x} \to \mathbf{x} + \mathbf{u}$

along coordinates $x_l = \{\mathbf{x}\}_l$. The nonlinear viscoelastic response, which includes the correlators $\eta_{ij;kl,mn}$, succinctly reads

$$J_{ij} = \eta_{ij;kl,mn} w_{kl} w_{mn}, \tag{2}$$

where J_{ij} is the nonlinear mass current. This is the viscoelastic analogue of the nonlinear electric current in response to electric fields E_k , $J_i = \sigma_{ijk} E_j E_k$, with nonlinear conductivity σ_{ijk} . The nonlinear viscoelastic effects map to the nonlinear electric transport effects upon replacing: $\eta_{ij;kl,mn} \to \sigma_{ijk}, J_{ij} \to J_i, w_{kl} \to E_k$. To characterize the NOVE, we consider tensor elements that are relevant to the dissipationless response, namely $\eta_{ii;jj,kk}$, $\eta_{ij;jk,ki}$ with $\{i,j,k\} = \{x,y,z\}$, schematics of which are presented in Fig. 1.

We find that the nonlinear viscoelastic tensor can be decomposed into gauge invariant two-state and three-state terms resolved over momentum space (see the End Matter for further technical details) as

$$\eta_{ij;kl,mn} = \int_{\mathbb{R}^{7}} d^{3}\mathbf{k} \left[\eta_{ij;kl,mn}^{2-\text{band}}(\mathbf{k}) + \eta_{ij;kl,mn}^{3-\text{band}}(\mathbf{k}) \right].$$
(3)

Here, we integrate over particle momenta \mathbf{k} in the three-dimensional Brillouin zone (BZ). The first term, $\eta_{ij;kl,mn}^{2-\mathrm{band}}(\mathbf{k})$, captures the two-band contributions to viscoelastic effects at zero temperature in systems with a finite energy gap, such as trivial and topological insulators. This measures the response arising from the quantum state geometry of virtual transitions of occupied states to the unoccupied state manifold induced by the stress tensor operator. The second term, $\eta_{ij;kl,mn}^{3-\mathrm{band}}(\mathbf{k})$, arises from the three-band contributions, which emerge from (i) triplets of virtual transitions between an occupied state and two virtual unoccupied energy levels and (ii) further contributions with two occupied states and one empty virtual energy level. Compactly, the momentum-local two-band contributions amount to

$$\eta_{ij;kl,mn}^{2-\text{band}}(\mathbf{k}) = 6 \sum_{\substack{a \in \text{occ} \\ b \in \text{unocc}}} \frac{1}{\Delta^{ba}} \Omega_{ij,(kl}^{ba} \partial_{mn}) \Delta^{ba}, \quad (4)$$

where $\partial_{kl} \equiv \partial/\partial w_{kl}$ are derivatives in strain, $\Delta^{ba} \equiv E^b_{\mathbf{k}} - E^a_{\mathbf{k}}$ are eigenstate energy differences and $\Omega^{ba}_{ij,mn} = \mathrm{i}[\langle \partial_{ij} u^a_{\mathbf{k}} | u^b_{\mathbf{k}} \rangle \langle u^b_{\mathbf{k}} | \partial_{mn} u^a_{\mathbf{k}} \rangle - \mathrm{c.c.}]$ is a symplectic form in the parameter space of deformations, and (\dots) denotes a normalized symmetrization of spatial index pairs. Here, we employ single-particle Bloch states satisfying the Schrödinger equation, $H |\psi^a_{\mathbf{k}}\rangle = E^a_{\mathbf{k}} |\psi^a_{\mathbf{k}}\rangle$, with the eigenvectors $|\psi^a_{\mathbf{k}}\rangle = e^{\mathrm{i}\mathbf{k}\cdot\mathbf{r}} |u^a_{\mathbf{k}}\rangle$ and position operator \mathbf{r} . The three-band contributions read

$$\eta_{ij;kl,mn}^{3-\text{band}}(\mathbf{k}) = 12 \left(\sum_{\substack{a \in \text{occ} \\ b,c \in \text{unocc} \\ b < c}} - \sum_{\substack{a \in \text{unocc} \\ b,c \in \text{occ} \\ b < c}} \right) \frac{\Delta^{cb}}{\Delta^{ba} \Delta^{ac}}$$

$$\times \operatorname{Re}\left[\Delta^{cb}Q_{(ij,kl,mn)}^{abc} + \Delta^{ba}Q_{ij,(kl,mn)}^{cab} + \Delta^{ac}Q_{ij,(kl,mn)}^{bca}\right],\tag{5}$$

with $Q_{ij,kl,mn}^{abc} = A_{ij}^{ac} A_{kl}^{cb} A_{mn}^{ba}$ and $A_{ij}^{ab} = \mathrm{i} \left\langle u_{\mathbf{k}}^{a} \middle| \partial_{ij} u_{\mathbf{k}}^{b} \right\rangle$. Here, $Q_{ij,kl,mn}^{abc}$ and A_{ij}^{ab} are extensions of the three-state quantum geometric tensor [64, 65] and of the non-Abelian Berry connection, respectively. The three-state geometric tensor captures the amplitudes of interband transitions between three states [25, 41, 64], which reflects the nonlinear character of the odd viscoelastic effect. For full derivations of $\eta_{ij;kl,mn}^{2-\mathrm{band}}(\mathbf{k})$, $\eta_{ij;kl,mn}^{3-\mathrm{band}}(\mathbf{k})$ and a detailed symmetry analysis of these terms, see the Supplemental Material (SM) [66].

Example I: Nonlinear viscoelasticity of Hopf bands.— We now turn to concrete model settings to exemplify the controllable effect in two topological bands. The NOVE under consideration requires inherently threedimensional quantum geometry, which mixes all three spatial dimensions, and breaks multiple symmetries (see SM [66]). Thus, we appeal to basic three-dimensional models of magnetic topological insulators with nontrivial topologies which naturally provide nontrivial quantum geometries [67]. To this end, consider an extended twoband Moore-Ren-Wen (MRW) Hopf insulator model [68], see End Matter. The integer topological Hopf invariant, $\chi \in \mathbb{Z}$, reads: $\chi = -\frac{1}{4\pi^2} \int_{\text{BZ}} d^3 \mathbf{k} \, \varepsilon^{ijk} A_i^{aa} \Omega_{jk}^{aa}$, with $\Omega_{jk}^{aa} = \partial_{kj} A_k^{aa} - \partial_{kk} A_j^{aa}$ the band-diagonal Berry curvature tensor. The Berry curvature tensors inherited from the invariant naturally provide for $\eta_{ij;kl,mn}^{2-\text{band}}$, as we demonstrate in Fig. 2. Here, we can access an arbitrarily high strate in Fig. 2. Here, we can access an arbitrarily high Hopf invariant upon a $k_z \to pk_z$ scaling, with $p \in \mathbb{Z}$ [69]. Furthermore, we may control topological phases across TPTs by varying a topological mass parameter m. In Fig. 2, we show the changes and the integer (p) scaling of the $\eta_{xx;yy,zz}$, $\eta_{yy;zz,xx}$ nonlinear viscoelastic tensor components. Notably, the trivial phase realizes negligibly small odd viscoelastic effects, unlike its topological counterparts.

Example II: Multiband nonlinear viscoelasticity.— We now focus on the demonstration of the multiband contribution, $\eta_{ij;kl,mn}^{3-{\rm band}}$, as shown in Fig. 2. As a starting point, we adapt chiral three-dimensional models in Altland–Zirnbauer class AIII [49]. We stress that the retrieved effect is, however, intrinsically geometric in nature, and goes beyond nontrivial topologies per se. In particular, the effect appears under perturbations that strictly break the invariant. As an example, we can further illustrate the effect in flattened chiral models with perturbations. The perturbations are necessary, as any system with \mathcal{T} , \mathcal{PT} and momentum-space $\mathcal{M}_{ij}\mathcal{T}$ realizes a vanishing response (see SM [66]), and both the MRW and (unperturbed) chiral model possess a combined mirror-time-reversal $\mathcal{M}_{ij}\mathcal{T}$ symmetry for appropriate i, j = x, y, z. The band flattening ensures the isolation of geometric effects from those of dissipation, a feature unique to the three-band contribution. In this light, we start with flattened perturbed three-band systems characterized by a chiral invariant, $\nu_i \in \mathbb{Z}$, [70, 71], see End Matter.

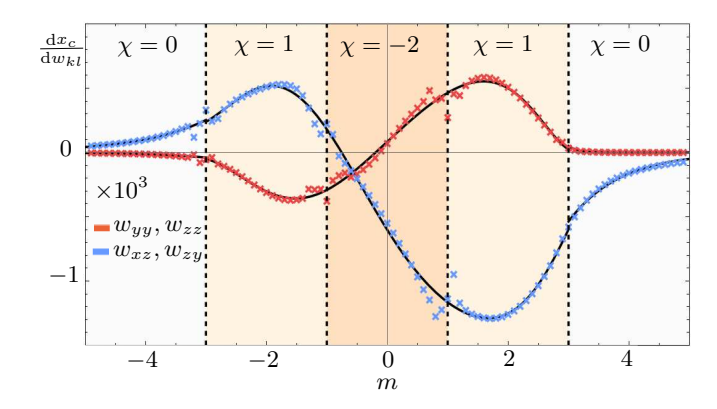


FIG. 3. Real-space representation of the NOVE in the perturbed MRW model for $\chi=1$ and $\delta=1/2$, see End Matter. Rate of change of Wannier center x-coordinate x_c with equal normal-stresses w_{yy}, w_{zz} (red) and equal shear-stresses w_{xz}, w_{zy} (blue), depicted as a function of mass parameter m. The plots show the net current in the x direction, which admits gradients in the y direction for the shear-stress response. The viscoelastic response of the Wannier functions changes across TPTs, displaying correspondence to the hydrodynamics derived in the momentum-space formalism.

We observe that analogously to the NOVE driven by $\eta_{ij;kl,mn}^{2-{\rm band}},$ the quantitative scaling of the response function $\eta_{ij;kl,mn}$ given by the multiband term $\eta_{ij;kl,mn}^{3-{\rm band}}$ drastically changes across the TPTs, see Fig. 2(c). However, we find that the strength of the three-band contribution is orders of magnitude smaller than the values arising from $\eta_{ij;kl,mn}^{2-{\rm band}}.$ We attribute this discrepancy to the inherent dependence of $\eta_{ij;kl,mn}^{2-\text{band}}$ on the band dispersion, the effect of which we nullify in $\eta_{ij;kl,mn}^{3-\text{band}}$ by flattening the bands. Moreover, we note that the multiband NOVE vanishes at high mass parameters |m|, as the multistate geometric tensors Q_{jln}^{abc} are suppressed in this regime. While this chiral setup effectively demonstrates the geometric nature of the effect, we further note in passing that the three-band effect can also be retrieved in models with a preserved invariant, analogously to the two-band Hopf case. Indeed, when all bands are gapped and characterized by a classifying space $U(3)/U(1)^3$, this allows for an integer invariant $(\pi_3[U(3)/U(1)^3] = \mathbb{Z})$ that does not rely on additional symmetries beyond translational symmetry and particle conservation symmetry [67, 72].

Nonlinear viscoelasticity in Wannier basis.— Having retrieved the two-band and three-band viscoelastic momentum-space contributions in topological and geometrically nontrivial phases, we now characterize the NOVE in the real-space formalism. Correspondingly, we demonstrate how the nonlinear viscoelastic effects are manifested in the real-space Wannier function representation. To this end, we transform the single-particle states to the localized Wannier basis $|a\mathbf{R}\rangle = \int_{\mathrm{BZ}} \frac{\mathrm{d}^3\mathbf{k}}{(2\pi)^3} \, e^{-\mathrm{i}\mathbf{k}\cdot\mathbf{R}} \, |\psi^a_{\mathbf{k}}\rangle$ [73, 74], and deduce their centers of mass $x_c \equiv \langle a\mathbf{0}|\,\hat{x}\,|a\mathbf{0}\rangle$ for the lowest band a=1,

subject to perturbations w_{kl}, w_{mn} .

In Fig. 3, we show the normal- and shear-stress induced Wannier velocities $\mathrm{d}x_c/\mathrm{d}w_{kl}$ in different topological phases, which are consistent with the particle mass currents J_{ij} shown in Fig. 1. Hence, we show that the localized wavepacket basis reflects the nonlinear odd viscoelastic transport induced by the deformations, consistently with the values of nonlinear response functions $\eta_{ij;kl,mn}$ demonstrated in Fig. 2. As such, we show that the NOVE naturally arises in momentum-space and real-space representations of fermionic wavefunctions realizing three-dimensional quantum-state geometries.

Discussion and conclusion.— The dissipationless character of the NOVEs combining all three spatial directions is expected, given that the retrieved effects can be thought of as the viscoelastic counterparts of the widely studied electronic nonlinear Hall effects. Notably, although for the electromagnetic responses which are analogous to uniaxial strains, there always exists a coordinate choice such that $\sigma_{xyz} = 0$, the same is not applicable for biaxial strains [75]. This stems from different behaviours of uniaxial and biaxial strains under addition, and that the tensorial representation of the nonlinear correlators under consideration mixes all three directions twice. This yields a geometric nontrivial response present beyond particular coordinate frames, following the transformation of geometric tensors present in Eqs. (4), (5). We further note that, consistently with the numerical results, there is an analytical correspondence between normalstress $(\eta_{xx;yy,zz})$ and shear-stress $(\eta_{yx;zy,xz},\eta_{zx;yz,xy})$ responses shown in Fig. 1. A rigorous proof of the intrinsic dependence of distinct nonlinear viscoelastic tensor components is given in the SM [66].

It should be stressed that, unlike the linear odd viscoelasticity, the nonlinear viscoelastic effects realize a unique interplay of two-state and three-state contributions. The vanishing of the three-band term under different symmetries reflects the chirality of the electronic ground state. These physical implications arise from the fact that the three-state tensors manifest in the skewness of the Wannier functions [76]. In particular, the three-band contribution $\eta^{3-\text{band}}_{ij;kl,mn}$ is intrinsically three-dimensional, due to the symmetries of the three-state quantum geometric tensor Q^{abc}_{ijk} . Moreover, in this interpretation, we found that increasing the values of these quantum geometric tensors, and thus the skewness and chirality of the Wannier states, enables the strains and shears to couple more strongly, within a direct proportionality to the higher geometric tensors.

We further comment on the implementation of strain in both the theoretical and experimental contexts of nonlinear viscous effects. For second-order responses, the adapted Peierls gauge formalism for strains and stress tensors, $T_{ij} = \partial H/\partial w_{ij} = -k_i \partial H/\partial k_j$ [63, 77] is justified. This follows from the fact that T_{ij} evaluated at $w_{ij} = 0$ allows to neglect the higher Hamiltonian derivatives proportional to $w_{ab}w_{cd}$ (see SM [66]). In this context, we note that the higher-order derivative terms survive in the $w_{ab} \rightarrow 0$ limit, analogously to the nonlinear electromagnetic responses. However, for third-order nonlinear viscoelastic effects, which are beyond the scope of this work, this approximation would not suffice to capture the viscoelastic phenomenology correctly. We further note that the vanishing of $\eta_{ij;kl,mn}$ under different symmetries follows directly from the representation theory of higher-rank tensors, independently of the approximations used.

Finally, we address how to isolate the nonlinear viscoelastic effects experimentally. To realize NOVEs, a protocol to generate shear forces should be adapted similarly to linear responses [10, 13]. However, in the presence of nontrivial $\eta_{ij;kl,mn}$ correlators, the scaling of the current response would be expected to deviate from linear. The degree of nonlinearity, combined with the transverse character of the response of systems subject to biaxial strain, e.g., w_{xx}, w_{yy} , should precisely reflect the qualitative phenomenological features of the odd effects identified in this work. Concerning material candidates, we anticipate that magnetic topological insulators, e.g., axion insulators, could naturally realize NOVEs, due to the three-dimensional multiband quantum geometry accessible in these phases. Consequently, effective θ -vacua of axion insulators within realistic material setups [78–80] provide for a promising route to not only generate, but also amplify NOVE responses. Finally, we note that from a theoretical angle, the formulation of the effect suggests that generalizations to higher dimensions, with N-band terms, provides a fruitful avenue for further studies.

In summary, we uncovered a class of exotic nonlinear odd viscoelastic effects. We showed that these effects naturally arise in magnetic three-dimensional topological phases, and also in topologically trivial phases with nontrivial three-dimensional and three-state quantum geometries. Hence the response, if measured in a bulk material, provides an experimental fingerprint for the intrinsic quantum state geometries of higher geometric tensors and unconventional topological invariants. Furthermore, our work, which focuses on dc nonlinear viscoelastic effects, paves the way for further studies of analogous time-dependent responses. We leave the characterization of time-dependent nonlinear and odd viscoelastic responses, as well as the resultant exotic phenomenology, for future theoretical and experimental works.

Acknowledgments.— The authors thank Joe Huxford and Giandomenico Palumbo for illuminating discussions. A.J. acknowledges funding from the School of Natural Sciences, University of Manchester. W.J.J. acknowledges funding from the Rod Smallwood Studentship at Trinity College, Cambridge. M.M. was funded by an EPSRC ERC underwrite Grant No. EP/X025829/1. R.-J.S. acknowledges funding from an EPSRC ERC underwrite Grant No. EP/X025829/1, and a Royal Society exchange Grant No. IES/R1/221060, as well as Trinity College, Cambridge.

- L. D. Landau and E. M. Lifshitz, Fluid Mechanics, 2nd ed., Course of Theoretical Physics, Vol. 6 (Pergamon Press, Oxford, 1987).
- [2] L. D. Landau and E. M. Lifshitz, Theory of Elasticity, 3rd ed., Course of Theoretical Physics, Vol. 7 (Butterworth-Heinemann, 1986).
- [3] D. Tong, Kinetic theory notes, https://www.damtp.cam.ac.uk/user/tong/kintheory/kintheory.pdf.
- [4] D. Banerjee, A. Souslov, A. G. Abanov, and V. Vitelli, Odd viscosity in chiral active fluids, Nature Communications 8, 1573 (2017).
- [5] B. Offertaler and B. Bradlyn, Viscoelastic response of quantum Hall fluids in a tilted field, Phys. Rev. B 99, 035427 (2019).
- [6] C. Scheibner, A. Souslov, D. Banerjee, P. Surówka, W. T. M. Irvine, and V. Vitelli, Odd elasticity, Nature Physics 16, 475–480 (2020).
- [7] M. Fruchart, C. Scheibner, and V. Vitelli, Odd viscosity and odd elasticity, Annual Review of Condensed Matter Physics 14, 471 (2023).
- [8] S. Chen, X. M. de Wit, M. Fruchart, F. Toschi, and V. Vitelli, Odd viscosity suppresses intermittency in direct turbulent cascades, Phys. Rev. Lett. 133, 144002 (2024).
- [9] J. E. Avron, R. Seiler, and P. G. Zograf, Viscosity of quantum Hall fluids, Phys. Rev. Lett. 75, 697 (1995).
- [10] C. Hoyos and D. T. Son, Hall viscosity and electromagnetic response, Phys. Rev. Lett. 108, 066805 (2012).
- [11] B. Bradlyn, M. Goldstein, and N. Read, Kubo formulas for viscosity: Hall viscosity, Ward identities, and the relation with conductivity, Phys. Rev. B 86, 245309 (2012).
- [12] P. Rao and B. Bradlyn, Hall viscosity in quantum systems with discrete symmetry: Point group and lattice anisotropy, Phys. Rev. X 10, 021005 (2020).
- [13] A. I. Berdyugin, S. G. Xu, F. M. D. Pellegrino, R. Krishna Kumar, A. Principi, I. Torre, M. Ben Shalom, T. Taniguchi, K. Watanabe, I. V. Grigorieva, M. Polini, A. K. Geim, and D. A. Bandurin, Measuring Hall viscosity of graphene's electron fluid, Science 364, 162–165 (2019).
- [14] M. Sherafati, A. Principi, and G. Vignale, Hall viscosity and electromagnetic response of electrons in graphene, Phys. Rev. B 94, 125427 (2016).
- [15] R. B. Laughlin, Anomalous quantum Hall effect: An incompressible quantum fluid with fractionally charged excitations, Phys. Rev. Lett. 50, 1395 (1983).
- [16] Q. Niu, D. J. Thouless, and Y.-S. Wu, Quantized hall conductance as a topological invariant, Phys. Rev. B 31, 3372 (1985).
- [17] K. von Klitzing, The quantized Hall effect, Rev. Mod. Phys. 58, 519 (1986).
- [18] H. L. Stormer, Nobel lecture: The fractional quantum Hall effect, Rev. Mod. Phys. 71, 875 (1999).
- [19] R. Yu, W. Zhang, H.-J. Zhang, S.-C. Zhang, X. Dai, and Z. Fang, Quantized anomalous Hall effect in magnetic topological insulators, Science 329, 61–64 (2010).
- [20] N. Read and E. H. Rezayi, Hall viscosity, orbital spin, and geometry: Paired superfluids and quantum Hall systems, Phys. Rev. B 84, 085316 (2011).
- [21] N. Nagaosa, J. Sinova, S. Onoda, A. H. MacDonald, and N. P. Ong, Anomalous Hall effect, Rev. Mod. Phys. 82,

- 1539 (2010).
- [22] Y. Gao, S. A. Yang, and Q. Niu, Field Induced Positional Shift of Bloch Electrons and Its Dynamical Implications, Phys. Rev. Lett. 112, 166601 (2014).
- [23] I. Sodemann and L. Fu, Quantum nonlinear Hall effect induced by Berry curvature dipole in time-reversal invariant materials, Phys. Rev. Lett. 115, 216806 (2015).
- [24] C. Wang, Y. Gao, and D. Xiao, Intrinsic Nonlinear Hall Effect in Antiferromagnetic Tetragonal CuMnAs, Phys. Rev. Lett. 127, 277201 (2021).
- [25] W. J. Jankowski and R.-J. Slager, Quantized integrated shift effect in multigap topological phases, Phys. Rev. Lett. 133, 186601 (2024).
- [26] H. Liu, J. Zhao, Y.-X. Huang, W. Wu, X.-L. Sheng, C. Xiao, and S. A. Yang, Intrinsic Second-Order Anomalous Hall Effect and Its Application in Compensated Antiferromagnets, Phys. Rev. Lett. 127, 277202 (2021).
- [27] N. Wang, D. Kaplan, Z. Zhang, T. Holder, N. Cao, A. Wang, X. Zhou, F. Zhou, Z. Jiang, C. Zhang, S. Ru, H. Cai, K. Watanabe, T. Taniguchi, B. Yan, and W. Gao, Quantum-metric-induced nonlinear transport in a topological antiferromagnet, Nature 621, 487–492 (2023).
- [28] A. Gao, Y.-F. Liu, J.-X. Qiu, B. Ghosh, T. V. Trevisan, Y. Onishi, C. Hu, T. Qian, H.-J. Tien, S.-W. Chen, M. Huang, D. Bérubé, H. Li, C. Tzschaschel, T. Dinh, Z. Sun, S.-C. Ho, S.-W. Lien, B. Singh, K. Watanabe, T. Taniguchi, D. C. Bell, H. Lin, T.-R. Chang, C. R. Du, A. Bansil, L. Fu, N. Ni, P. P. Orth, Q. Ma, and S.-Y. Xu, Quantum metric nonlinear Hall effect in a topological antiferromagnetic heterostructure, Science 381, 181–186 (2023).
- [29] C. Ortix, Nonlinear Hall Effect with Time-Reversal Symmetry: Theory and Material Realizations, Adv. Quantum Technol. 4, 2100056 (2021).
- [30] T. Ideue and Y. Iwasa, Symmetry breaking and nonlinear electric transport in van der Waals nanostructures, Annu. Rev. Condens. Matter Phys. 12, 201 (2021).
- [31] Z. Du, H.-Z. Lu, and X. Xie, Nonlinear Hall effects, Nature Reviews Physics 3, 744 (2021).
- [32] D. Kaplan, T. Holder, and B. Yan, General nonlinear Hall current in magnetic insulators beyond the quantum anomalous Hall effect, Nature Communications 14, 294 (2023).
- [33] N. Nagaosa and Y. Yanase, Nonreciprocal transport and optical phenomena in quantum materials, Annu. Rev. Condens. Matter Phys. 15, 63 (2024).
- [34] S. Shim, M. Mehraeen, J. Sklenar, S. S.-L. Zhang, A. Hoffmann, and N. Mason, Spin-polarized antiferromagnetic metals, Annu. Rev. Condens. Matter Phys. 16 (2025).
- [35] M. Suárez-Rodríguez, F. De Juan, I. Souza, M. Gobbi, F. Casanova, and L. E. Hueso, Nonlinear transport in non-centrosymmetric systems, Nature Materials 24, 1005 (2025).
- [36] C.-P. Zhang, J. Xiao, B. T. Zhou, J.-X. Hu, Y.-M. Xie, B. Yan, and K. T. Law, Giant nonlinear Hall effect in strained twisted bilayer graphene, Phys. Rev. B 106, L041111 (2022).
- [37] A. Jain, W. J. Jankowski, and R.-J. Slager, Anomalous geometric transport signatures of topological Euler class, Phys. Rev. B 111, 235149 (2025).

- [38] S. Klevtsov and P. Wiegmann, Geometric adiabatic transport in quantum Hall states, Phys. Rev. Lett. 115, 086801 (2015).
- [39] F. Xie, Z. Song, B. Lian, and B. A. Bernevig, Topology-bounded superfluid weight in twisted bilayer graphene, Phys. Rev. Lett. 124, 167002 (2020).
- [40] J. Ahn, G.-Y. Guo, and N. Nagaosa, Low-frequency divergence and quantum geometry of the bulk photovoltaic effect in topological semimetals, Phys. Rev. X 10, 041041 (2020).
- [41] J. Ahn, G.-Y. Guo, N. Nagaosa, and A. Vishwanath, Riemannian geometry of resonant optical responses, Nature Physics 18, 290–295 (2021).
- [42] A. Bouhon, A. Timmel, and R. Slager, Quantum geometry beyond projective single bands (2023), arXiv:2303.02180 [cond-mat.mes-hall].
- [43] M. A. Oancea, T. B. Mieling, and G. Palumbo, Quantum geometric tensors from sub-bundle geometry (2025), arXiv:2503.17163 [math-ph].
- [44] J. Provost and G. Vallee, Riemannian structure on manifolds of quantum states, Communications in Mathematical Physics 76, 289 (1980).
- [45] W. J. Jankowski, R.-J. Slager, and M. Pizzochero, Enhancing the hyperpolarizability of crystals with quantum geometry, Phys. Rev. Lett. 135, 126606 (2025).
- [46] P. Törmä, S. Peotta, and B. A. Bernevig, Superconductivity, superfluidity and quantum geometry in twisted multilayer systems, Nature Reviews Physics 4, 528 (2022).
- [47] P. Törmä, Essay: Where can quantum geometry lead us?, Phys. Rev. Lett. 131, 240001 (2023).
- [48] F. D. M. Haldane, Model for a quantum Hall effect without Landau levels: Condensed-matter realization of the "parity anomaly", Phys. Rev. Lett. 61, 2015 (1988).
- [49] A. Kitaev, Periodic table for topological insulators and superconductors, AIP Conference Proceedings 1134, 22 (2009).
- [50] C.-K. Chiu, J. C. Y. Teo, A. P. Schnyder, and S. Ryu, Classification of topological quantum matter with symmetries, Rev. Mod. Phys. 88, 035005 (2016).
- [51] J. Kruthoff, J. de Boer, J. van Wezel, C. L. Kane, and R. Slager, Topological classification of crystalline insulators through band structure combinatorics, Phys. Rev. X 7, 041069 (2017).
- [52] H. C. Po, A. Vishwanath, and H. Watanabe, Symmetrybased indicators of band topology in the 230 space groups, Nature Communications 8, 50 (2017).
- [53] B. Bradlyn, L. Elcoro, J. Cano, M. G. Vergniory, Z. Wang, C. Felser, M. I. Aroyo, and B. A. Bernevig, Topological quantum chemistry, Nature 547, 298 (2017).
- [54] Y. X. Zhao and Y. Lu, PT-symmetric real dirac fermions and semimetals, Phys. Rev. Lett. 118, 056401 (2017).
- [55] A. Bouhon, A. M. Black-Schaffer, and R.-J. Slager, Wilson loop approach to fragile topology of split elementary band representations and topological crystalline insulators with time-reversal symmetry, Phys. Rev. B 100, 195135 (2019).
- [56] A. Bouhon, Q. Wu, R. Slager, H. Weng, O. V. Yazyev, and T. Bzdušek, Non-Abelian reciprocal braiding of Weyl points and its manifestation in ZrTe, Nature Physics 16, 1137 (2020).
- [57] A. Bouhon, T. Bzdusek, and R. Slager, Geometric approach to fragile topology beyond symmetry indicators, Phys. Rev. B 102, 115135 (2020).

- [58] J. Ahn, S. Park, and B.-J. Yang, Failure of Nielsen-Ninomiya Theorem and Fragile Topology in Two-Dimensional Systems with Space-Time Inversion Symmetry: Application to Twisted Bilayer Graphene at Magic Angle, Phys. Rev. X 9, 021013 (2019).
- [59] J. Ahn, S. Park, D. Kim, Y. Kim, and B.-J. Yang, Stiefel-Whitney classes and topological phases in band theory, Chinese Physics B 28, 117101 (2019).
- [60] Z. Davoyan, W. J. Jankowski, A. Bouhon, and R.-J. Slager, Three-dimensional PT-symmetric topological phases with a Pontryagin index, Phys. Rev. B 109, 165125 (2024).
- [61] W. J. Jankowski, A. S. Morris, Z. Davoyan, A. Bouhon, F. N. Ünal, and R.-J. Slager, Non-Abelian Hopf-Euler insulators, Phys. Rev. B 110, 075135 (2024).
- [62] C. W. Chau, W. J. Jankowski, and R.-J. Slager, Optical signatures of Euler superconductors, Phys. Rev. B 112, 064512 (2025).
- [63] H. Shapourian, T. L. Hughes, and S. Ryu, Viscoelastic response of topological tight-binding models in two and three dimensions, Phys. Rev. B 92, 165131 (2015).
- [64] M. Mehraeen, Quantum response theory and momentumspace gravity, Phys. Rev. Lett. 135, 156302 (2025).
- [65] Z. Guo, Z. Lu, H. Wang, and K. Chang, Bicircular lightinduced multistate geometric current, Phys. Rev. B 112, 035162 (2025).
- [66] See the Supplemental Material (SM) for the derivation of nonlinear odd viscoelastic effects (Sec. I), expansion of stress operators (Sec. II), symmetry analysis (Sec. III), and for numerical details (Sec. IV). The Supplemental Material includes Refs. [81–88].
- [67] W. J. Jankowski, R.-J. Slager, and G. Palumbo, Probing tensor monopoles and gerbe invariants in three-dimensional topological matter (2025), arXiv:2507.22116 [cond-mat.mes-hall].
- [68] J. E. Moore, Y. Ran, and X.-G. Wen, Topological surface states in three-dimensional magnetic insulators, Phys. Rev. Lett. 101, 186805 (2008).
- [69] A. Alexandradinata, A. Nelson, and A. A. Soluyanov, Teleportation of Berry curvature on the surface of a Hopf insulator, Phys. Rev. B 103, 045107 (2021).
- [70] T. Neupert, L. Santos, S. Ryu, C. Chamon, and C. Mudry, Noncommutative geometry for threedimensional topological insulators, Phys. Rev. B 86, 035125 (2012).
- [71] G. Palumbo and N. Goldman, Tensor Berry connections and their topological invariants, Phys. Rev. B 99, 045154 (2019).
- [72] B. Lapierre, T. Neupert, and L. Trifunovic, N-band hopf insulator, Phys. Rev. Res. 3, 033045 (2021).
- [73] N. Marzari and D. Vanderbilt, Maximally localized generalized Wannier functions for composite energy bands, Phys. Rev. B 56, 12847 (1997).
- [74] N. Marzari, A. A. Mostofi, J. R. Yates, I. Souza, and D. Vanderbilt, Maximally localized Wannier functions: Theory and applications, Rev. Mod. Phys. 84, 1419 (2012).
- [75] D. Socie and G. Marquis, *Multiaxial fatigue* (SAE international, 1999).
- [76] A. Avdoshkin, J. Mitscherling, and J. E. Moore, Multistate geometry of shift current and polarization, Phys. Rev. Lett. 135, 066901 (2025).
- [77] M. R. Hirsbrunner, O. Dubinkin, F. J. Burnell, and

- T. L. Hughes, Anomalous crystalline-electromagnetic responses in semimetals, Phys. Rev. X 14, 041060 (2024).
- [78] R. S. K. Mong, A. M. Essin, and J. E. Moore, Antiferromagnetic topological insulators, Phys. Rev. B 81, 245209 (2010).
- [79] M. M. Otrokov, I. I. Klimovskikh, H. Bentmann, D. Estyunin, A. Zeugner, Z. S. Aliev, S. Gaß, A. U. B. Wolter, A. V. Koroleva, A. M. Shikin, M. Blanco-Rey, M. Hoffmann, I. P. Rusinov, A. Y. Vyazovskaya, S. V. Eremeev, Y. M. Koroteev, V. M. Kuznetsov, F. Freyse, J. Sánchez-Barriga, I. R. Amiraslanov, M. B. Babanly, N. T. Mamedov, N. A. Abdullayev, V. N. Zverev, A. Alfonsov, V. Kataev, B. Büchner, E. F. Schwier, S. Kumar, A. Kimura, L. Petaccia, G. Di Santo, R. C. Vidal, S. Schatz, K. Kißner, M. Ünzelmann, C. H. Min, S. Moser, T. R. F. Peixoto, F. Reinert, A. Ernst, P. M. Echenique, A. Isaeva, and E. V. Chulkov, Prediction and observation of an antiferromagnetic topological insulator, Nature 576, 416 (2019).
- [80] N. H. Jo, L.-L. Wang, R.-J. Slager, J. Yan, Y. Wu, K. Lee, B. Schrunk, A. Vishwanath, and A. Kaminski, Intrinsic axion insulating behavior in antiferromagnetic MnBi₆Te₁₀, Phys. Rev. B 102, 045130 (2020).
- [81] H. Rostami, M. I. Katsnelson, G. Vignale, and M. Polini, Gauge invariance and Ward identities in nonlinear response theory, Annals of Physics 431, 168523 (2021).
- [82] J. Sipe and A. Shkrebtii, Second-order optical response in semiconductors, Phys. Rev. B 61, 5337 (2000).
- [83] Y. Michishita and R. Peters, Effects of renormalization and non-Hermiticity on nonlinear responses in strongly correlated electron systems, Phys. Rev. B 103, 195133 (2021).
- [84] F. de Juan, A. G. Grushin, T. Morimoto, and J. E. Moore, Quantized circular photogalvanic effect in Weyl semimetals, Nature Communications 8, 15995 (2017).
- [85] D. E. Parker, T. Morimoto, J. Orenstein, and J. E. Moore, Diagrammatic approach to nonlinear optical response with application to Weyl semimetals, Phys. Rev. B 99, 045121 (2019).
- [86] O. Matsyshyn and I. Sodemann, Nonlinear Hall acceleration and the quantum rectification sum rule, Phys. Rev. Lett. 123, 246602 (2019).
- [87] S. Tsirkin and I. Souza, On the separation of Hall and Ohmic nonlinear responses, SciPost Phys. Core 5, 039 (2022).
- [88] D. Mandal, S. Sarkar, K. Das, and A. Agarwal, Quantum geometry induced third-order nonlinear transport responses, Phys. Rev. B 110, 195131 (2024).

END MATTER

Details on models with NOVE.— In the following, we further detail the constructions and exact parametrizations of model Hamiltonians realizing NOVEs. We begin with a two-band Hopf insulator model which admits an adaptable tight-binding representation in real space [68]. The two-band Hamiltonian can be expressed as $H_0 = \mathbf{d} \cdot \boldsymbol{\sigma}$, with $d_i = \mathbf{z}^{\dagger} \sigma_i \mathbf{z}$ and a vector \mathbf{z} that induces the Hopf invariant,

$$\mathbf{z} = \begin{pmatrix} \sin(ak_x) + i\sin(ak_y) \\ \sin(ak_z) + i\left(\sum_i \cos(ak_i) - m\right) \end{pmatrix}. \tag{6}$$

Here, **z** realizes nontrivial Hopf invariant $\chi=1$ for 1<|m|<3 and $\chi=-2$ for |m|<1. However, the presence of the k-space $\mathcal{M}_{xz}\mathcal{T}$ symmetry notably causes the response to vanish in this model (see SM [66]), to which end we add a perturbation

$$\Delta H = \delta \sin[a(k_x + k_z)]\sigma_z,\tag{7}$$

with a perturbation strength δ within a combined Hamiltonian, $H = H_0 + \Delta H$.

For the three-band model, we begin with the model defined which possess an invariant protected by chiral symmetry [71]. The Hamiltonian reads $H = \mathbf{d} \cdot \boldsymbol{\lambda}$, with $\mathbf{d} = [0,0,0,\sin(ak_x),\sin(ak_y),\sin(ak_z),m-\sum_i\cos(ak_i),0]^{\mathrm{T}}$, where i=x,y,z, and $\boldsymbol{\lambda}$ is the 8-vector of Gell-Mann matrices that represents a basis of 3×3 Hermitian traceless matrices. In order to isolate the three-band contribution, we set the energies of this model explicitly to (-1,0,1). This flat-band limit causes the energy derivatives, and thus the two-band terms, to vanish. This model, however, still possesses a k-space $\mathcal{M}_{yz}\mathcal{T}$ symmetry, which nullifies the response. Similar to the two-band model, we add a three-band perturbation

$$\Delta H = \delta \sin[a(k_x + k_z)]\lambda_1,\tag{8}$$

which breaks the chiral symmetry and trivializes the chiral invariant ν_i , but retains the nontrivial geometry of the unperturbed model.

SUPPLEMENTAL MATERIAL Nonlinear Odd Viscoelastic Effect

Ashwat Jain, 1, * Wojciech J. Jankowski, 2, † M. Mehraeen, 1 and Robert-Jan Slager 1, 2, ‡

¹Department of Physics and Astronomy, University of Manchester, Oxford Road, Manchester M13 9PL, UK ²TCM Group, Cavendish Laboratory, University of Cambridge, J. J. Thomson Avenue, Cambridge CB3 0HE, UK (Dated: December 1, 2025)

CONTENTS

I.	Derivation of the nonlinear odd viscoelastic responses	2
II.	Expansion of the stress operators	5
III.	Symmetry analysis	5
IV.	Numerical details	7
	References	7

^{*} ashwat.jain@postgrad.manchester.ac.uk

[†] wjj25@cam.ac.uk

[‡] robert-jan.slager@manchester.ac.uk

I. DERIVATION OF THE NONLINEAR ODD VISCOELASTIC RESPONSES

We begin by deriving the general Kubo-like response to second order, following Refs. [1] and [2]. For an observable A(t), whose expectation value we are interested in for a system governed by a Hamiltonian perturbation $H(t) = \sum_{i=1}^{2} B_i(t)\phi_i(t)$, we write

$$\langle A(t) \rangle = \langle \psi(t) | A(t) | \psi(t) \rangle$$

$$= \langle \psi_0 | U^{\dagger}(t) A(t) U(t) | \psi_0 \rangle, \qquad (1)$$

where U(t) is the time evolution operator

$$U(t) = T \exp\left(-i \int_{-\infty}^{t} dt' H(t')\right),\tag{2}$$

and T is the time ordering operator. Using the Dyson series truncated to second order [3]

$$U(t) \approx 1 - i \int_{-\infty}^{t} dt' H(t') - \int_{-\infty}^{t} dt' \int_{-\infty}^{t'} dt'' H(t') H(t''), \tag{3}$$

we expand Eq. (1). This reads [1]

$$A(t) = \langle A(t) \rangle + \sum_{i=1}^{2} \int_{-\infty}^{\infty} d\tau_{1} \chi_{A;B_{i}}(t;\tau_{1}) \phi(t-\tau_{1})$$

$$+ \sum_{i,j=1}^{2} \int_{-\infty}^{\infty} d\tau_{1} \int_{-\infty}^{\infty} d\tau_{2} \chi_{A;B_{i},B_{j}}(t;\tau_{1},\tau_{2}) \phi_{i}(t-\tau_{1}) \phi_{j}(t-\tau_{2}),$$
(4)

where

$$\chi_{A;B_i}(t;\tau_1) = i\Theta(\tau_1)\langle [B_i(t-\tau_1), A(t)]\rangle,\tag{5}$$

$$\chi_{A;B_{i},B_{i}}(t;\tau_{1},\tau_{2}) = i^{2}\Theta(\tau_{2}-\tau_{1})\Theta(\tau_{1})\langle [B_{i}(t-\tau_{2}), [B_{i}(t-\tau_{1}), A(t)]]\rangle.$$
(6)

In Fourier space (Lehmann representation), the second order response function $\chi_{A;B_1,B_2}$ reads [1]

$$\chi_{A;B_{1},B_{2}}(\omega',\omega_{1},\omega_{2}) = \frac{1}{2}\delta(\omega'-\omega_{1}-\omega_{2})\left[\sum_{a,b,c} \frac{A^{ac}B_{2}^{cb}B_{1}^{ba}}{\omega'^{+}+\Delta^{ac}} \left(\frac{P^{ab}}{\omega_{1}^{+}+\Delta^{ab}} - \frac{P^{bc}}{\omega_{1}^{+}+\Delta^{bc}}\right) + (B_{1},\omega_{1}) \leftrightarrow (B_{2},\omega_{2})\right],\tag{7}$$

where a, b, c are the Hamiltonian eigenstate (band) indices, $\omega_{1,2}^+ = \omega_{1,2} + i\eta_{1,2}$, the matrix element $\langle a|O|b\rangle$ is written as O^{ab} for brevity, $\Delta^{ab} = E^a - E^b$, and $P^{ab} = P^a - P^b$ with $P^b = \langle b|P|b\rangle = \mathrm{e}^{-\beta E^b}/\mathcal{Z}$, and finally \mathcal{Z} is the partition function at temperature $1/\beta$. Throughout this work, we use indices a, b, c to denotes bands and indices i, j, k, l, m, n as coordinate indices.

We can use this to define the conductivity $\sigma_{A;B_1,B_2}$ as [4]

$$\sigma_{A;B_1,B_2} = \frac{-i\omega'^+}{i\omega_1^+ i\omega_2^+} \chi_{A;B_1,B_2}.$$
 (8)

The frequency denominators are required when our perturbation fields are gauge potentials [5, 6] (i.e., when we are working in minimal coupling or velocity gauge - which we will, for the stress responses). They do not appear while working in the length gauge [7]. The frequency numerator stems from the fact that χ as we have calculated is a polarization susceptibility, as opposed to a current density response. Since current density is just the time derivative of the polarization, the equivalent relation in Fourier space picks up a factor of $-i\omega^+$. Indeed, we are interested in the momentum current when our perturbations are the stresses within the Peierls gauge substitution (minimal coupling of distortion to momenta) of Ref. [8], and these external frequency factors are important.

Next, we wish to extract the odd (dissipationless) component of our conductivity $\sigma_{A:B_1,B_2}$. Correspondingly, we write [9]

$$\sigma^{\text{odd}} = \sigma^{\text{tot}} - \sigma^{\text{Ohmic}},\tag{9}$$

where the Ohmic (dissipative) conductivity is the fully symmetrized version with respect to all its operators. In the linear case this simply yields

$$\sigma_{A;B_i}^{\text{odd}} = \sigma_{A;B_i}^{\text{tot}} - \sigma_{(A;B_i)}^{\text{Ohmic}} = \sigma_{[A;B_i]},\tag{10}$$

i.e., the antisymmetrized version. This decomposition of the total conductivity into odd and dissipative parts is well-established in literature [9, 10]. For the nonlinear case, the response partitioning is not as straightforward, and we write

$$\sigma_{A;B_1,B_2}^{\text{odd}} = \sigma_{A;B_i,B_2}^{\text{tot}} - \sigma_{(A;B_1,B_2)}^{\text{Ohmic}}.$$
(11)

Since our response functions are already symmetric in the inputs B_1 and B_2 , we can write this as

$$\sigma_{A;B_{1},B_{2}}^{\text{odd}} = \sigma_{A;(B_{i},B_{2})}^{\text{tot}} - \frac{1}{3} (\sigma_{A;(B_{1},B_{2})}^{\text{tot}} + \sigma_{B_{1};(A,B_{2})}^{\text{tot}} + \sigma_{B_{2};(B_{1},A)}^{\text{tot}})$$

$$= \frac{1}{3} (2\sigma_{A;(B_{1},B_{2})}^{\text{tot}} - \sigma_{B_{1};(A,B_{2})}^{\text{tot}} - \sigma_{B_{2};(B_{1},A)}^{\text{tot}}), \tag{12}$$

where $\sigma_{P;(Q,R)}$ is the already-symmetrized form which uses the response function symmetric in its inputs, Eq. (7). Next, since we are interested in the dc response to purely static fields ϕ_i , we take the symmetric dc limit $\omega_1 = \omega_2 \rightarrow 0$ (See Ref. [11], Sec. VI A, with $n_a = n_b = 1/2$). The antisymmetric limit is more appropriate for optical responses, where it represents a rectification [12] to the zero-frequency divergences, and is related to the circular photogalvanic effect (CPGE) [13]. In this symmetric frequency limit, the expression for the odd conductivity reads

$$\sigma_{A;B_{1},B_{2}}^{\text{odd}} = \lim_{\omega \to 0} \frac{2i}{\omega^{+}} \Big[\chi_{A;B_{1},B_{2}}(2\omega,\omega,\omega) - \chi_{B_{1};A,B_{2}}(2\omega,\omega,\omega) - \chi_{B_{2};B_{1},A}(2\omega,\omega,\omega) \Big]. \tag{13}$$

We consider the case of n bands $|1\rangle, |2\rangle \dots |n\rangle$ at zero temperature with integer filling, restricting our attention to clean systems. This gives us $P^a = 0$ if the band energy E^a is above the Fermi level, and $P^a = 1$, if it is below. We take the symmetric limit $\omega_1 = \omega_2 = \omega'/2 \equiv \omega$. Under these assumptions, we can perform the sum over eight terms in Eq. (7) (of which two, that correspond to all bands a, b, c, filled and empty, vanish identically) to get a simplified expression:

$$\sigma_{A;B_1,B_2}^{\text{odd}} = \lim_{\omega^+ \to 0} \frac{\mathrm{i}}{\omega} \left(\sum_{\substack{a \in \text{unocc.} \\ b,c \in \text{unocc.} \\ b,r \in \text{occ.}}} - \sum_{\substack{a \in \text{unocc.} \\ b,r \in \text{occ.} \\ c}} \right) \left[\frac{1}{\Delta^{ca} \Delta^{ba}} \left(\frac{S^{acb}}{(1 - \frac{2\omega^+}{\Delta^{ca}})(1 - \frac{\omega^+}{\Delta^{ba}})} + \frac{S^{cba}}{(1 + \frac{\omega^+}{\Delta^{ca}})(1 - \frac{\omega^+}{\Delta^{ba}})} + \frac{S^{bac}}{(1 + \frac{\omega^+}{\Delta^{ca}})(1 - \frac{\omega^+}{\Delta^{ba}})} \right) \right], \quad (14)$$

where

$$S^{abc} = \frac{1}{3} \left(2 \langle a|A|b \rangle \langle b|B_1|c \rangle \langle c|B_2|a \rangle - \langle a|B_1|b \rangle \langle b|A|c \rangle \langle c|B_2|a \rangle - \langle a|B_2|b \rangle \langle b|B_1|c \rangle \langle c|A|a \rangle \right) + (B_1 \leftrightarrow B_2). \tag{15}$$

We note here that the two sums in Eq. (14) represent the electron and hole contributions. Next, in order to take the limit, we expand the denominators in small ω and collect terms by powers of ω , noting that the energy differences are nonvanishing everywhere for a gapped phase. This yields

$$\sigma_{A;B_{1},B_{2}}^{\text{odd, dc}} = \lim_{\omega \to 0} \frac{\mathrm{i}}{\omega^{+}} \left(\sum_{\substack{a \in \text{occ.} \\ b,c \in \text{unocc.}}} - \sum_{\substack{a \in \text{unocc.} \\ b,c \in \text{occ.}}} \right) \left[\frac{S^{acb} + S^{cba} + S^{bac}}{\Delta^{ca} \Delta^{ba}} + \omega^{+} \frac{\Delta^{ba} (2S^{acb} - S^{cba} - S^{bac}) - \Delta^{ca} (2S^{bac} - S^{acb} - S^{cba})}{(\Delta^{ca})^{2} (\Delta^{ba})^{2}} + \mathcal{O}(\omega^{2}) \right].$$

$$(16)$$

We note now that Eq. (15) implies

$$S^{acb} + S^{cba} + S^{bac} = 0, (17)$$

which nullifies the divergent term in Eq. (16). We also use this identity to simplify the numerator of the next term and write

$$\sigma_{A;B_1,B_2}^{\text{odd,dc}} = 3i \left(\sum_{\substack{a \in \text{orc.} \\ b \in \text{curred}}} - \sum_{\substack{a \in \text{uncc.} \\ b \in \text{core}}} \right) \left(\frac{\Delta^{ba} S^{acb} - \Delta^{ca} S^{bac}}{(\Delta^{ca})^2 (\Delta^{ba})^2} \right), \tag{18}$$

upon taking the zero-frequency limit ($\omega \to 0$).

We now specialize to the case of elastic perturbations, using the approach in Ref. [8]. To obtain the viscosity $\eta_{ij;kl,mn}$, we substitute $A \to \tilde{T}_{ij}, B_1 \to \tilde{T}_{kl}, B_2 \to \tilde{T}_{mn}$, where

$$\tilde{T}_{ij} = \frac{\partial H}{\partial w_{ij}} \tag{19}$$

is the generalized force (stress) operator, $w_{ij} = \partial_i u_j$ is the distortion (unsymmetrized strain) tensor [8], and i, j, k, l, m, n represent spatial indices. We implement strain by gauging momenta using a generalized Peierls substitution [8]

$$k_j \to k_j - w_{ij} \frac{\sin(k_i a)}{a},$$
 (20)

which allows us to write (denoting by ∂_i the derivative with respect to k_i)

$$\tilde{T}_{ij} = -\frac{\sin(k_i a)}{a} \partial_j H,\tag{21}$$

where a denotes the lattice constant of the system. This yields

$$\langle a|A|b\rangle\langle b|B_1|c\rangle\langle c|B_2|a\rangle = -\frac{1}{a^3}\sin(ak_i)\sin(ak_k)\sin(ak_m)\langle a|\partial_jH|b\rangle\langle b|\partial_lH|c\rangle\langle c|\partial_nH|a\rangle. \tag{22}$$

Further, we can use

$$\langle a|\partial_j H|b\rangle = \partial_j E^b \langle a|b\rangle + \Delta^{ba} \langle a|\partial_j b\rangle$$

= $\partial_j E^b \delta^{ab} - i\Delta^{ba} A_j^{ab},$ (23)

where the non-Abelian Berry connection is defined as $A_j^{ab} = i \langle a | \hat{\partial}_j b \rangle$, and we assume orthonormal orbitals. Clearly, if a = b, this yields only the energy derivative (since Δ^{ba} vanishes), and if $a \neq b$, then only the non-Abelian Berry curvature term remains. We thus split into two cases, given the sums in Eq. (18): where b = c and where $b \neq c$, which we call the two-band and three-band contributions respectively. For the former, we obtain after some algebra

$$\eta_{ij;kl,mn}^{\text{odd, dc, }2-\text{band}} = \frac{6}{a^3} \sin(ak_i) \sin(ak_k) \sin(ak_m) \sum_{\substack{a \in \text{occ.} \\ b \in \text{unocc}}} \frac{1}{\Delta^{ba}} \left(\Omega_{j(l}^{ba} \partial_{n)} \Delta^{ba}\right), \tag{24}$$

where Ω_{jl}^{ba} is the symplectic curvature two-form defined as $\Omega_{jl}^{ba} = -2 \operatorname{Im}(A_j^{ba} A_l^{ab})$. On the other hand, the three-band contribution reads

$$\eta_{ij;kl,mn}^{\text{odd}, \text{dc}, 3-\text{band}} = \frac{12}{a^3} \sin(ak_i) \sin(ak_k) \sin(ak_m) \left(\sum_{\substack{a \in \text{occ.} \\ b, c \in \text{unocc.} \\ b \neq c}} - \sum_{\substack{a \in \text{unocc.} \\ b, c \in \text{occ.} \\ b \neq c}} \right) \left(\frac{\Delta^{cb}}{\Delta^{ba} \Delta^{ac}} \operatorname{Re} \left[\Delta^{cb} Q_{(jln)}^{abc} + \Delta^{ba} Q_{j(ln)}^{cab} + \Delta^{ac} Q_{j(ln)}^{bca} \right] \right), \tag{25}$$

where (...) represents a normalized symmetrization of index pairs, and we have used the definition of the three-state quantum geometric tensor [14]

$$Q_{jln}^{abc} = A_j^{ab} A_l^{bc} A_n^{ca}. (26)$$

Note that the symmetric part vanishes for both the two-band and three-band responses, allowing us to write

$$\eta_{ij;kl,mn}^{\text{odd, dc}} + \eta_{kl;mn,ij}^{\text{odd, dc}} + \eta_{mn;i,kl}^{\text{odd, dc}} = 0,$$
(27)

which shows explicitly that $\eta_{ij;kl,mn}^{\text{odd, dc}}$ is the nondissipative response component. Eq. (27) can also be interpreted as a sum rule for the response.

The factorizations of the sin(ak) terms can be recast in a more convenient form by defining the tensors

$$A_{ij}^{ab} \equiv i \left\langle u^a \middle| \partial_{w_{ij}} u^b \right\rangle, \tag{28}$$

$$\Omega_{ij,kl}^{ab} \equiv -2\operatorname{Im}(A_{ij}^{ab}A_{kl}^{ba}),\tag{29}$$

$$Q_{ij;kl,mn}^{abc} \equiv A_{ij}^{ab} A_{kl}^{bc} A_{mn}^{ca}. \tag{30}$$

(31)

These quantities can be thought of dressed versions of their pure quantum geometric counterparts, where momentum derivatives have been replaced by strain derivatives. Upon using the Peierls gauge substitution, Eq. (20), these quantities are related to their pure counterparts by simple multiplicative sine factors. We can also connect them to the stress tensor operators T_{ij} present in the correlators as: $A^{ab}_{ij} = \mathrm{i} \langle u^a | \partial H / \partial w_{ij} | u^b \rangle / \Delta^{ba} = \mathrm{i} \langle u^a | T_{ij} | u^b \rangle / \Delta^{ba}$, which can also be obtained by differentiating the Schrödinger equation with respect to the deformation fields w_{ij} . In terms of these quantities, the response functions take a simpler form:

$$\eta_{ij;kl,mn}^{\text{odd, dc, }2-\text{band}} = 6 \sum_{\substack{a \in \text{occ.} \\ b \in \text{unocc.}}} \Omega_{ij,(kl}^{ba} \partial_{mn}) \ln \Delta^{ba}, \tag{32}$$

$$\eta_{ij;kl,mn}^{\text{odd, dc, 3-band}} = 12 \left(\sum_{\substack{a \in \text{occ.} \\ b,c \in \text{unocc.} \\ b,c \in \text{cocc.}}} - \sum_{\substack{a \in \text{unocc.} \\ b,c \in \text{occ.} \\ b,c \in \text{occ.}}} \right) \left(\frac{\Delta^{cb}}{\Delta^{ba} \Delta^{ac}} \operatorname{Re} \left[\Delta^{cb} Q_{(ij,kl,mn)}^{abc} + \Delta^{ba} Q_{ij(kl,mn)}^{cab} + \Delta^{ac} Q_{ij(kl,mn)}^{bca} \right] \right), \tag{33}$$

where $\partial_{kl} \equiv \partial/\partial w_{kl}$. This way of expressing these quantities also elucidates that all responses which put the three directions on equal footing (i.e., responses which are either permutations of xx, yy, zz or of xy, yz, zx) must share the same form if their output index j is the same, since in Eqs. (24) and (25) one can redistribute the $\sin(ak_x)\sin(ak_y)\sin(ak_z)$ back into Ω and Q in any way of choice. We thus get

$$\eta_{xx;yy,zz}^{\text{odd,dc}} = \eta_{yx;zy,xz}^{\text{odd,dc}} = \eta_{zx;xy,yz}^{\text{odd,dc}}.$$
(34)

Further, due to the construction of σ , the symmetry between the swap of the last two index pairs is present, thus we have six equal η 's. Similarly we can swap around the indices for the yy; zz, xx and zz; xx, yy responses too, each yielding six equivalent η 's. Thus, the value of $\eta_{ij;kl,mn}$ for responses which place the three direction on equal footing is determined solely by the second index j. Combined with the sum rule of Eq. (27), this implies that there are two independent responses, for which we take the representatives xx; yy, zz and yy; zz, xx.

II. EXPANSION OF THE STRESS OPERATORS

In Ref. [5], it is shown that the definition of the total stress tensor as the metric variation of the action yields

$$T_{ij} = -\frac{\partial H}{\partial \lambda_{ij}}\Big|_{\Lambda=1},\tag{35}$$

where Λ is the unsymmetrized total strain tensor (called *e* in Ref. [8]) and λ is defined as

$$\Lambda = e^{\lambda}.\tag{36}$$

In Ref. [8], definitionally: $e_{ij} = \delta_{ij} = w_{ij}$. Altogether, this allows us to write

$$\partial \lambda = -\partial w + \mathcal{O}(w^2) \tag{37}$$

for small strains. This further leads to

$$T_{ij} = \frac{\partial H}{\partial w_{ij}} \Big|_{w=0},\tag{38}$$

which is precisely the form used in Ref. [8], and in the main text of this work. Importantly, it should be noted that the higher order terms vanish due to the condition $\Lambda = 1 \equiv \lambda = 0 \equiv w = 0$, and so Eq. (38) is exact.

III. SYMMETRY ANALYSIS

The results for the two-band and three-band nonlinear contributions to the dissipationless viscosity tensor possess a high degree of symmetry, which we elucidate below. In particular, we show that the presence of \mathcal{T} , \mathcal{PT} or $\mathcal{M}_{ij}\mathcal{T}$ symmetries in the system cause the bulk response to vanish. Noting that time reversal (\mathcal{T}) symmetry acts by flipping all momentum components and complex conjugation, parity (\mathcal{P}) symmetry acts by flipping all momentum components and the k-space ij-mirror (\mathcal{M}_{ij}) symmetry acts by flipping momenta about the ij plane, we observe that under the presence of these symmetries the system obeys

$$\mathcal{T}: u(\mathbf{k}) = u^*(-\mathbf{k}) \qquad \Delta(\mathbf{k}) = \Delta(-\mathbf{k}), \tag{39}$$

$$\mathcal{PT}: u(\mathbf{k}) = u^*(\mathbf{k}). \tag{40}$$

$$\mathcal{M}_{xy}\mathcal{T}: u(k_x, k_y, k_z) = u^*(-k_x, -k_y, k_z) \qquad \Delta(k_x, k_y, k_z) = \Delta(-k_x, -k_y, k_z), \tag{41}$$

and similarly for $\mathcal{M}_{yz}\mathcal{T}$ and $\mathcal{M}_{zx}\mathcal{T}$. We now consider these symmetries one by one. Under \mathcal{T} , the off-diagonal Berry connection $A_j^{ab}(\mathbf{k}) = \mathrm{i} \left\langle u^a(\mathbf{k}) \middle| \partial_{k_j} u^b(\mathbf{k}) \right\rangle$ is forced to satisfy

$$A_i^{ab}(\mathbf{k}) = [A_i^{ab}(-\mathbf{k})]^*, \tag{42}$$

where * denotes complex conjugation. This in turn causes the interband symplectic Berry curvature forms, $\Omega_{jl}^{ab} = -2 \operatorname{Im}(A_j^{ab} A_l^{ba})$ [15], to be odd under \mathcal{T} ,

$$\Omega_{jl}^{ab}(\mathbf{k}) = -\Omega_{jl}^{ab}(-\mathbf{k}). \tag{43}$$

With a similar analysis, we can conclude that the three-state QGT $Q_{jln}^{abc} = A_j^{ab} A_l^{bc} A_n^{ca}$ follows

$$Q_{iln}^{abc}(\mathbf{k}) = [Q_{iln}^{abc}(-\mathbf{k})]^*, \tag{44}$$

showing that the real part of this tensor is even under \mathcal{T} . Further note that the factor $\sin(ak_i)\sin(ak_k)\sin(ak_m)$ and the momentum derivatives are both also odd under \mathcal{T} . In total, this behaviour of the geometric and algebraic quantities causes both the two-band response [Eq. (24)] and the three-band response [Eq. (25)] to follow

$$\eta(\mathbf{k}) = -\eta(-\mathbf{k}). \tag{45}$$

Thus, the integration over the BZ causes the bulk contribution to the viscosity to vanish in both cases.

Under the \mathcal{PT} symmetry, Eq. (39) implies that the off-diagonal Berry connection obeys

$$A_j^{ab}(\mathbf{k}) = -A_j^{ba}(\mathbf{k}),\tag{46}$$

which causes the interband Berry curvature (hence the two-band response) to vanish. On the other, the three-state QGT obeys

$$Q_{jln}^{abc}(\mathbf{k}) = -[Q_{jln}^{abc}(\mathbf{k})]^*. \tag{47}$$

However, noting that \mathcal{PT} symmetry implies real eigenvectors $u(\mathbf{k})$, the three-state QGT must be real, and this then implies that Q (and therefore the three-band response) is vanishing.

Finally, under $\mathcal{M}_{ij}\mathcal{T}$, we can perform a similar analysis. For concreteness, we consider the $\mathcal{M}_{xy}\mathcal{T}$ case below, though the argument remains unchanged for other mirror symmetries. We see from Eq. (41) that the off-diagonal Berry connection must satisfy

$$A_{x}^{ab}(k_{x}, k_{y}, k_{z}) = A_{x}^{ba}(-k_{x}, -k_{y}, k_{z}),$$

$$A_{y}^{ab}(k_{x}, k_{y}, k_{z}) = A_{y}^{ba}(-k_{x}, -k_{y}, k_{z}),$$

$$A_{z}^{ab}(k_{x}, k_{y}, k_{z}) = -A_{z}^{ba}(-k_{x}, -k_{y}, k_{z}).$$
(48)
$$(49)$$

Thus, the interband Berry curvature form satisfies

$$\Omega_{xy}^{ab}(k_x, k_y, k_z) = -\Omega_{xy}^{ab}(-k_x, -k_y, k_z),
\Omega_{yz}^{ab}(k_x, k_y, k_z) = \Omega_{yz}^{ab}(-k_x, -k_y, k_z),
\Omega_{zx}^{ab}(k_x, k_y, k_z) = \Omega_{zx}^{ab}(-k_x, -k_y, k_z).$$
(50)

(51)

On the other hand, the three-state QGT under $\mathcal{M}_{xy}\mathcal{T}$ can be shown to follow

$$Q_{jln}^{abc}(k_x, k_y, k_z) = -[Q_{jln}^{abc}(-k_x, -k_y, k_z)]^*,$$
(52)

as long as j, l, n take distinct values in $\{x, y, z\}$. This implies that the real part of Q is odd under $\mathcal{M}_{xy}\mathcal{T}$, and together with the fact that ∂_x and ∂_y are odd under $\mathcal{M}_{xy}\mathcal{T}$, while ∂_z and $\sin(ak_x)\sin(ak_y)\sin(ak_z)$ are even, we see that both two- and three-band contribution to the viscosity satisfy

$$\eta(k_x, k_y, k_z) = -\eta(-k_x, -k_y, k_z), \tag{53}$$

causing the response to vanish in every $k_x k_y$ plane on integration, and thus the bulk response is also vanishing.

With the above analysis, we see that the set of systems which can show a nonvanishing nonlinear odd viscoelastic effect precludes systems with \mathcal{T} , \mathcal{PT} or $\mathcal{M}_{ij}\mathcal{T}$ symmetries, and notably topological systems in classes AI, AII, BDI, CI, CII and DIII of the tenfold way. Amongst the remaining classes A, AIII, C and D, models which possess $\mathcal{M}_{ij}\mathcal{T}$ (such as the unperturbed chiral model presented in Ref. [16], which has $\mathcal{M}_{yz}\mathcal{T}$ symmetry) also have a vanishing nonlinear odd viscosity. The same argument forbids the classic MRW Hopf insulator model [17], which has $\mathcal{M}_{xz}\mathcal{T}$ symmetry, from showing this response. This was verified numerically for the unperturbed versions of both models discussed in the main text.

IV. NUMERICAL DETAILS

In this Section, we provide details of the numerical methods used to obtain Fig. 2 and Fig. 3 in the main text. First, a numerical estimate of the Hopf invariant for the perturbed MRW model was found using the construction presented in Ref. [18], as well as by numerically finding the preimage of two antipodal points on the two-sphere (S^2) under the Hopf map $\mathbf{d}(\mathbf{k})$ defined via

$$H(\mathbf{k}) = \mathbf{d}(\mathbf{k}) \cdot \boldsymbol{\sigma},\tag{54}$$

where σ is the vector of Pauli matrices. Both methods show in agreement that the Hopf invariant survives upon adding a perturbation of strength $0 \le \lambda \le 1$. Thus, λ was set to 1/2 for the plots.

All integrals for Fig. 3 in the main text were performed numerically over a discretized \mathbf{k} -grid. The presence of the Hopf invariant leads to an obstruction to a globally smooth periodic gauge, and Fig. 2 in the main text was obtained by computing Wannier functions in a maximally smooth (but non-periodic) gauge for a discretized \mathbf{k} -grid for every value of mass parameter m. For small applied strains, the position of the Wannier center was tracked with the derivative taken using a centered finite-difference over the strain points.

- [1] H. Rostami, M. I. Katsnelson, G. Vignale, and M. Polini, Gauge invariance and Ward identities in nonlinear response theory, Annals of Physics 431, 168523 (2021).
- [2] P. N. Butcher and D. Cotter, *The Elements of Nonlinear Optics*, Cambridge Studies in Modern Optics (Cambridge University Press, 1990).
- [3] H. Haber, The time evolution operator as a time-ordered exponential, https://scipp.ucsc.edu/~haber/ph215/TimeOrderedExp.pdf.
- [4] Here, we use conductivity in the general sense of response theory, not limiting ourselves to discussions of electrical conductivity. Later, we will specify the operators A, B_1 and B_2 to be stress operators corresponding to the case of viscosities.
- [5] B. Bradlyn, M. Goldstein, and N. Read, Kubo formulas for viscosity: Hall viscosity, Ward identities, and the relation with conductivity, Phys. Rev. B 86, 245309 (2012).
- [6] Y. Michishita and R. Peters, Effects of renormalization and non-Hermiticity on nonlinear responses in strongly correlated electron systems, Phys. Rev. B 103, 195133 (2021).
- [7] D. E. Parker, T. Morimoto, J. Orenstein, and J. E. Moore, Diagrammatic approach to nonlinear optical response with application to Weyl semimetals, Phys. Rev. B 99, 045121 (2019).
- [8] H. Shapourian, T. L. Hughes, and S. Ryu, Viscoelastic response of topological tight-binding models in two and three dimensions, Phys. Rev. B 92, 165131 (2015).
- [9] S. Tsirkin and I. Souza, On the separation of Hall and Ohmic nonlinear responses, SciPost Phys. Core 5, 039 (2022).
- [10] D. Mandal, S. Sarkar, K. Das, and A. Agarwal, Quantum geometry induced third-order nonlinear transport responses, Phys. Rev. B 110, 195131 (2024).
- [11] J. Sipe and A. Shkrebtii, Second-order optical response in semiconductors, Phys. Rev. B 61, 5337 (2000).
- [12] O. Matsyshyn and I. Sodemann, Nonlinear Hall acceleration and the quantum rectification sum rule, Phys. Rev. Lett. 123, 246602 (2019).
- [13] F. de Juan, A. G. Grushin, T. Morimoto, and J. E. Moore, Quantized circular photogalvanic effect in Weyl semimetals, Nature Communications 8, 15995 (2017).
- [14] M. Mehraeen, Quantum response theory and momentum-space gravity, Phys. Rev. Lett. 135, 156302 (2025).
- [15] J. Ahn, G.-Y. Guo, N. Nagaosa, and A. Vishwanath, Riemannian geometry of resonant optical responses, Nature Physics 18, 290–295 (2021).
- [16] G. Palumbo and N. Goldman, Tensor Berry connections and their topological invariants, Phys. Rev. B 99, 045154 (2019).
- [17] J. E. Moore, Y. Ran, and X.-G. Wen, Topological surface states in three-dimensional magnetic insulators, Phys. Rev. Lett. **101**, 186805 (2008).
- [18] W. J. Jankowski, R.-J. Slager, and G. Palumbo, Probing tensor monopoles and gerbe invariants in three-dimensional topological matter (2025), arXiv:2507.22116 [cond-mat.mes-hall].